

https://doi.org/10.1070/QEL16246

Ti:sapphire laser synchronised with femtosecond Yb pump laser via nonlinear pulse coupling in Ti:sapphire active medium

N.V. Didenko, A.V. Konyashchenko, D.A. Konyashchenko,
P.V. Kostryukov, I.I. Kuritsyn, A.P. Lutsenko, A.O. Mavritskiy

Abstract. **A laser system utilising the method of synchronous pumping of a Ti:sapphire laser by a high-power femtosecond Yb^{3+}-doped laser is described. The pulse repetition rate of the Ti:sapphire laser is successfully locked to the repetition rate of the Yb laser for more than 6 hours without the use of any additional electronics. The measured timing jitter is shown to be less than 1 fs. A simple qualitative model addressing the synchronisation mechanism utilising the cross-phase modulation of oscillation and pump pulses within a Ti:sapphire active medium is proposed. Output parameters of the Ti:sapphire laser as functions of its cavity length are discussed in terms of this model.**

Keywords: *synchronous pumping, femtosecond pumping, Ti:sapphire laser, cross-phase modulation.*

1. Introduction

Femtosecond laser systems using sapphire crystals doped with titanium ions have become widespread as the main instrument in numerous fields of research. In this connection, much attention is paid to the synchronisation and control of a time delay between the pulses generated by lasers of this class and other optical sources. A few approaches to the solution of this problem exist using, e.g., the active medium or other nonlinear element, common for two laser cavities [1–3], the optical schemes with cavity loss modulation of a laser source with the radiation of the other one [4], the electronic feedback circuits [5–7], as well as the synchronous pumping method.

The synchronous pumping method has been widely used in laser oscillators based on dye solutions, allowing the reduction of pulse duration in these sources [8, 9]. Individual attempts of using this technique in other types of laser oscillators have also been made [10, 11], including Ti:sapphire lasers [12–16]. In the latter case, the pumping was implemented using picosecond pulses, which provided the automatic initiation of the mode-locking operation in the pumped laser. This approach was also considered as an alternative to the continuous-wave pumping of the Ti:sapphire crystal with gas (argon ion) and solid-state lasers, generating the radiation in the green spectral region. Until now the possibility of synchronous pumping of Ti:sapphire lasers with the pulses having the duration of the order of a hundred femtoseconds was not a subject of appropriate attention in spite of additional advantages offered by this method.

At present, the importance of synchronous pumping of the Ti:sapphire active medium is related to the development of high-power solid-state IR lasers [17, 18], generating pulses of subpicosecond duration. Since the 60% energy conversion efficiency into the second harmonic is possible for such a source, its average output power (7–8 W) is sufficient to produce no less than 0.5 W of average power at the Ti:sapphire laser output.

The method of femtosecond synchronous pumping possesses the following advantages as compared to the pumping with continuous-wave radiation:

– Automatic initiation of the mode-locking operation in the Ti:sapphire laser without the use of a saturable absorber or an additional triggering device.

– Reduction of the pump laser cost due to its simplification, caused by a high efficiency of conversion of pulsed radiation into the second harmonic (no intracavity frequency doubling in the pumping laser is necessary).

In the case, the pulse repetition rates (PRRs) of the pump and Ti:sapphire laser differ by more than 100 Hz, the parameters of the Ti:sapphire laser radiation are similar to those for the case of cw pumping. The modulation depth of the Ti:sapphire laser output power at the difference frequency between the pump and oscillation repetition rates does not exceed 0.1% in this case [12].

Compared to picosecond pulsed pumping, the femtosecond one allows automatic and precise locking (within millihertz) of the Ti:sapphire laser pulse repetition rate to that of the pump laser, provided that the difference of cavity lengths is sufficiently small ($\sim$1 μm).

The locking of the lasers is due to the nonlinear coupling between the short pump pulses having a high peak power and the oscillation pulses inside the Ti:sapphire rod. High-efficiency cross-phase modulation (XPM) of oscillation and short pump pulses co-propagating in the medium with high third order nonlinearity gives rise to the efficient temporal 'attraction' of the pulses in the presence of net negative cavity dispersion [19–21]. As shown by a simple qualitative analysis, this effect occurs due to the asymmetric spectral broadening of the oscillation pulses because of XPM.

In the present paper, we describe the method of locking the PRR of a femtosecond laser to that of its pump by using synchronous pumping and propose a qualitative model of the pulse repetition rate locking mechanism. In addition, we

N.V. Didenko, A.V. Konyashchenko, P.V. Kostryukov, A.P. Lutsenko
P.N. Lebedev Physics Institute, Russian Academy of Sciences,
Leninskiy prosp. 53, 119991 Moscow, Russia;
e-mail: abrown@yandex.ru;
D.A. Konyashchenko, I.I. Kuritsyn, A.O. Mavritskiy Avesta Ltd.,
ul. Fizicheskaya 11, Troitsk, 108840 Moscow, Russia;
e-mail: eli@avesta.ru

Received 3 November 2016
Kvantovaya Elektronika **47** (1) 7–13 (2017)
Translated by V.L. Derbov

briefly describe an experimental system, utilising this method to obtain pulse trains that are locked in frequency and phase.

2. Frequency locking mechanism under synchronous pumping

The locking mechanism of the Ti:sapphire laser PRR to the PRR of the pump laser in the plane-wave approximation for co-propagating pump and oscillation pulses can be described by the equation

$$\frac{\partial A_g}{\partial z} + k_1(\omega_g)\frac{\partial A_g}{\partial t} + \frac{ik_2(\omega_g)}{2}\frac{\partial^2 A_g}{\partial t^2} + \frac{\alpha}{2}A_g = i\gamma_g |A_g|^2 A_g + 2i\gamma_g |A_p|^2 A_g, \quad (1)$$

where A_g is the slowly varying amplitude of the Ti:sapphire oscillation field within the laser rod, normalised so that $|A_g|^2$ equals the instantaneous power of the optical radiation at the given frequency ω_g; A_p is the analogous quantity, characterising the given pump field; k_1 and k_2 are the coefficients of the power series expansion of the wavenumber $k(\omega)$ around ω_g; α is the coefficient of nonresonant medium absorption; and γ_g is the nonlinearity coefficient depending on the effective area of the field modes A_p and A_g (for which the transverse distributions in the crystal practically coincide).

The first term in the right-hand side of Eqn (1) allows for the self-action of the intracavity Ti:sapphire oscillation, in particular, self-phase modulation (SPM). The second term is responsible for XPM.

Note that this equation is applicable only under a considerable number of assumptions. We do not take into account the dispersion pulse broadening in the crystal, since for our experimental conditions the dispersion length (~20 cm) for both the pump and oscillation pulse is much greater than the length of the crystal. Neglecting the nonresonant absorption of the oscillation [the term $(\alpha/2)A_g$ in Eqn (1)] we obtain the following expression for the correction to the instantaneous frequency of the oscillation field caused by the action of pumping:

$$\delta\omega_{CPM} = -2\gamma_g \frac{\partial |A_p|^2}{\partial t} z = -\frac{n_2\omega_g}{c}\frac{\partial I_p}{\partial t} z, \quad (2)$$

where I_p is the pump field intensity, and n_2 is the nonlinear refractive index. The interaction between the pump and oscillation pulses in the Ti:sapphire crystal leads to a local decrease in the phase velocity of the oscillation wave, proportional to the intensity of the pump field, which results in a change in the oscillation pulse duration and the centre frequency of its spectrum. If the oscillation pulse is initially ahead of the pump pulse (i.e., located in the region $\eta \leqslant 0$ in the coordinate frame moving with the group velocity of the pump pulse, see Fig. 1), then its trailing edge slows down under the influence of the pump pulse. The pulse therefore stretches, gains a negative chirp, and its carrier frequency decreases. If the oscillation pulse lags compared to the pump pulse, it also gains a negative chirp, but the pulse is compressed, and its carrier frequency grows as it propagates through the crystal.

Due to the shift of the oscillation pulse carrier frequency, according to Eqn (2) in the first approximation of the dispersion theory, the pulse group velocity changes, which leads to a change in the pulse roundtrip time in the cavity having length l. Provided that the total roundtrip cavity dispersion is negative,

$$\frac{\partial u}{\partial \omega}\Big|_{\omega=\omega_g} = -\frac{u^2}{l}\frac{\partial^2 \Phi}{\partial \omega^2} > 0,$$

the change in the average group velocity u of the oscillation pulse is

$$\Delta u = -\frac{n_2\omega_g}{c} z \frac{dI_p}{dt}\frac{\partial u}{\partial \omega}\Big|_{\omega=\omega_g}. \quad (3)$$

Equation (3) implies that if the oscillation pulse lags slightly behind the pump pulse and overlaps with its descending edge, i.e., $\partial I_p/\partial\eta < 0$, then the centre wavelength of the oscillation field decreases and, therefore, the group velocity of the oscillation pulse in the cavity increases. Therefore, at the next roundtrip of the cavity the lag of the oscillation pulse relative to the pump pulse becomes smaller, i.e., in a few axial periods the efficient attraction between the pulses occurs. If the oscillation pulse outstrips the pump pulse, then the described mechanism operates in the opposite direction, which finally leads to efficient stabilisation of the time delay between the peaks of the pulses [20].

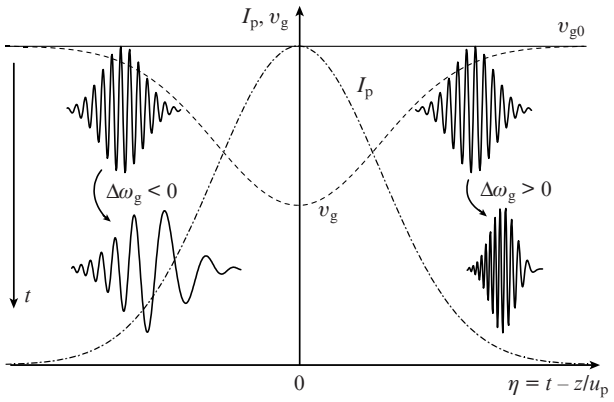

Figure 1. Variation in duration and frequency ($\Delta\omega_g$) of the generated pulse in the Ti:sapphire crystal under the influence of the pump field. The dash-dotted curve is the pump pulse intensity envelope in the coordinate frame moving with the group velocity u_p. The dashed curve shows the local phase velocity of the oscillation radiation $v_g = v_{g0} + \Delta v_g(I_p)$. The vertical arrow shows the direction of the evolution of the oscillation pulse in time. The illustration of the evolution of pulses does not allow for the difference of group velocities for the pump and oscillation pulses in the crystal and for their absorption.

3. Description of experiment

The above effect of delay stabilisation between the pulses of the Ti:sapphire laser and the pump laser was observed experimentally, as well as the accompanying shift of the oscillation carrier frequency, arising as a response of the system to the change in the repetition rate difference between the lasers. To perform the experiment, we constructed a prototype of the system, consisting of two laser oscillators assembled on a common optical water-cooled plate and protected from the ambient environment by a large casing. In the system, an ytterbium-doped solid-state IR TeMa-1050 laser (Avesta-Project) was used together with the optical second harmonic generator (SHG) providing up to 4.2 W of

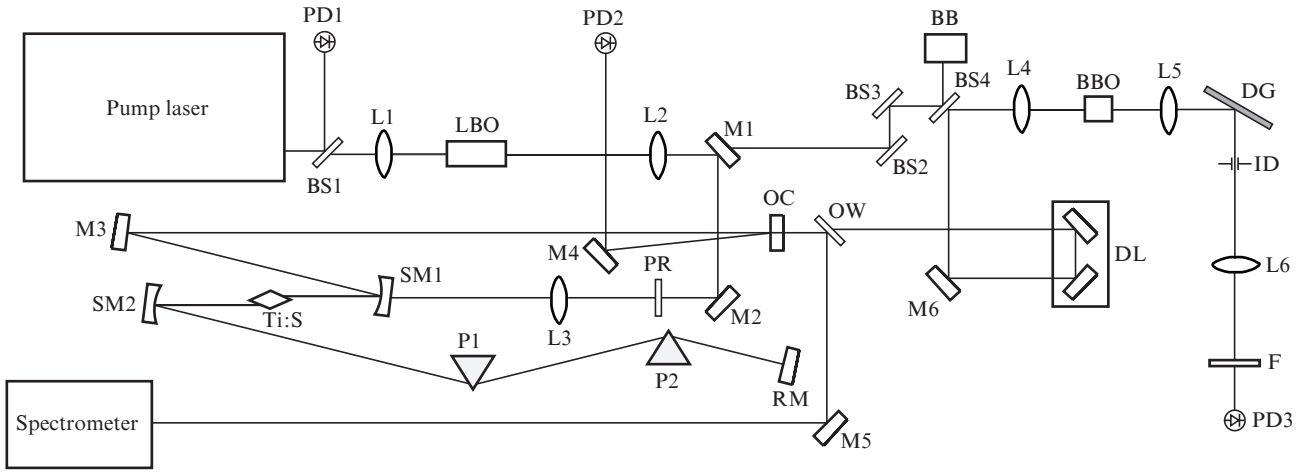

Figure 2. Optical scheme of the system of oscillators with synchronous pumping and the schematic diagram of the experiment on measuring the temporal fluctuations between the pulses of these oscillators: (BS1 – BS4) beam splitters for the wavelength 1050 nm; (L1 – L6) focusing lenses; (BB) beam blocker; (M1 and M2) dielectric mirrors for the wavelength 525 nm; (PR) polarisation rotator; (SM1 and SM2) spherical mirrors; (Ti : S) sapphire crystal doped with titanium ions; (P1 and P2) compressor prisms; (RM) retra-reflecting mirror with dielectric coating; (M3 – M6) dielectric mirrors for the wavelength 800 nm; (OC) output coupler; (OW) output window of the Ti : sapphire laser; (PD1 – PD3) photodetectors based on pin-photodiodes; (DL) motorised delay line; (LBO) nonlinear lithium triborate crystal; (BBO) nonlinear barium beta-borate crystal; (DG) 1800 grooves mm^{-1} diffraction grating; (ID) iris diaphragm; (F) blue-green glass filter.

power at 525 nm with a pulse duration of 170 fs and a pulse repetition rate of 70 MHz in the train. The output of the SHG was used to pump the Ti : sapphire laser (Fig. 2) after polarisation rotation and focusing into the crystal of the active medium. The fundamental frequency of the ytterbium laser radiation was separated from the second harmonic by mirror M1 and directed to a circuit detecting the delay between the pulses of two laser trains (it is located to the right of the output window OW of the Ti : sapphire laser in Fig. 2).

The synchronously pumped laser had an asymmetric Z-shaped cavity with the Ti : sapphire crystal and a prism compressor. The Ti : sapphire laser radiated 25 – 60 fs pulses (depending on its configuration and tuning) at the centre wavelength 800 nm. The average output power of the Ti : sapphire oscillator was 300 mW at the pulse repetition rate 70 MHz. In the compressor arm of the cavity the movable mirror RM was installed (Fig. 2) on a piezoelectric stepper motor.

The displacement of the movable mirror leads to the variation in the cavity length of the Ti : sapphire laser, which provides controllable variation of its pulse repetition rate within a wide range (~1 MHz) with respect to the PRR of the pump laser. By automated stepwise correction of the movable mirror RM position, the laser cavity length was maintained with sufficient accuracy to provide steady locking of the Ti : sapphire PRR to that of the pump laser. The shift of the centre wavelength of the radiation generated by the Ti : sapphire laser relative to the wavelength in the regime of asynchronous or continuous-wave pumping served as the error signal. The current centre wavelength was calculated in real time from the readings of a spectrometer integrated in the system. By choosing the feedback system sensitivity to the values of the spectral shift the compensation for the slow drift of the cavity length of the Ti : sapphire laser and, as a consequence, its exact locking with the pump laser was provided for a long time.

To determine the precision of PRR locking of two lasers we used a cross-correlation sum frequency generation scheme (Fig. 2) [22]. The timing jitter between the pulse trains of the pump laser and the Ti : sapphire oscillator was measured using this scheme. Because of the specific features of the optical setup, the jitter was measured between the pulse of the pump laser and the nearest following pulse of the Ti : sapphire oscillator. The delay line DL allows the measurement of the correlation function of the pulses, the FWHM parameter of which can be used to estimate the jitter between the pulse trains [23]. If the pulses from both lasers arrive at the detector (the crystal of the sum frequency generator) with a delay, corresponding to the overlap of their envelopes nearly at the half-maximum level, the sum frequency signal is proportional to the jitter between the pulses [2].

4. Results and discussion

4.1. Synchronous pumping experiment

If the difference between the pulse repetition rates of the femtosecond pump laser and the Ti : sapphire oscillator exceeds a few hundred hertz, then, from the point of view of the active medium excitation, the operation regime of the Ti : sapphire laser does not differ in principle from the case of pumping with a continuous-wave green laser. This conclusion is confirmed by the closeness of the values of such characteristics as the average power, the pulse duration and the radiation spectrum of the Ti : sapphire laser, measured under pulsed and continuous-wave pumping. The oscilloscopic observation of the envelope of a continuous train of pulses from a synchronously pumped Ti : sapphire laser does not reveal a visible amplitude modulation if the difference of cavity lengths is sufficiently large. The insensitivity of the amplitude of pulses of the Ti : sapphire laser to the pulsed character of the pump is due to a large relaxation time of the upper laser energy level compared to the pump pulse train period. One can observe this insensitivity under pumping a Ti : sapphire laser with both femtosecond and picosecond pulses [12, 16].

Figure 3 shows the PRR difference between the Ti : sapphire laser (f_2) and the pump laser (f_1) as a function of the

cavity length mismatch $\Delta x = l_2 - l_1$ (l_1 and l_2 are the cavity lengths of the pump laser and the Ti:sapphire laser, respectively). One can select three regions in Fig. 3. The first region is located in the interval $\Delta x = -0.5 \div 1.0$ μm, where f_2 is exactly locked to f_1. The second region corresponds to the interval $\Delta x = -4.2 \div 4.8$ μm, outside the first region, where frequency locking is still supported but does not have the feature of auto initiation like in the first region. The third region is the region of amplitude-modulated continuous oscillation.

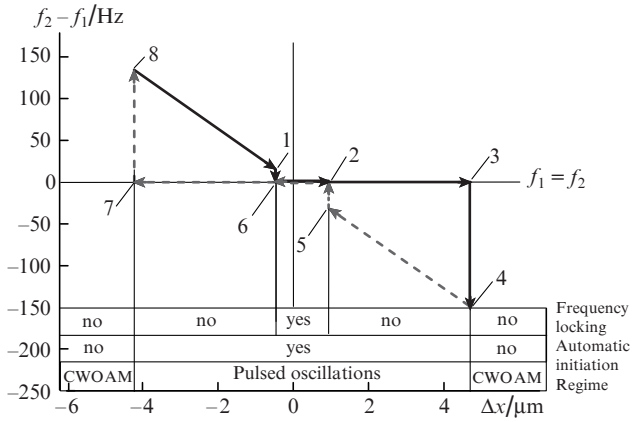

Figure 3. Detuning of the pulse repetition rate f_2 for the Ti:sapphire laser from the rate f_1 of the pump pulses as a function of difference of cavity lengths towards the cavity elongation (solid arrows) and shortening (dashed arrows) of the cavity. CWO AM is the regime of continuous-wave oscillation of the Ti:sapphire laser, characterised by the presence of amplitude modulation with the frequency f_1.

The automatic initiation of the femtosecond oscillation regime with simultaneous automatic pulling of the pulse repetition rate to that of the pump pulses f_1 occurs in the Ti:sapphire oscillator, the cavity length of which lies in the first region. If the femtosecond oscillation regime is interrupted by an external factor, the automatic restart of the femtosecond oscillation occurs at $f_1 = f_2$ (frequency locking). The variations in the cavity length of the Ti:sapphire laser within the first region are accompanied by the shift of the centre wavelength of the oscillation spectrum that compensates for the difference Δx, so that the exact matching between f_2 and f_1 is preserved. In our experiment, similar to the earlier publication [24], we observed a linear correspondence between the shift of the centre oscillation wavelength of the Ti:sapphire laser and the change in its cavity length (Fig. 4). The sign of the slope of the corresponding graph confirms the negative total dispersion in the laser cavity, which agrees with our qualitative model. When the length of the Ti:sapphire laser cavity is increased, the compensating shift of its oscillation spectrum occurs towards shorter wavelengths, since the group velocity of the oscillation pulse in this case increases (see also Ref. [18]).

In the second region, we observed the automatic initiation of the femtosecond oscillation regime in the Ti:sapphire laser, after a short perturbation of its cavity. However, the lock-in of the pulse repetition rate f_2 (pulling of f_2 to the frequency f_1) after disrupting the oscillation regime does not occur automatically; therefore, the dependence $f_2(\Delta x)$ turns into a line with the slope, corresponding to the regime of continuous-wave pumping of the Ti:sapphire oscillator. When the transition from the first region to the second one occurs

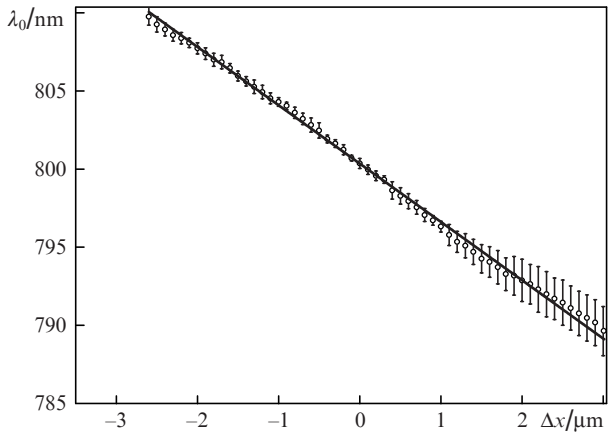

Figure 4. Dependence of the centre wavelength λ_0 of the radiation spectrum of the Ti:sapphire laser on the length of its cavity in the regime of permanent locking with the pump laser (points). Solid line shows the approximation of the dependence with the linear function $y = a + bx$, where $a = 800.34 \pm 0.03$ and $b = -3.73 \pm 0.02$. The deviations from the straight line are due to the periodic variation in temperature of the optical plate, on which the laser system is assembled.

without disturbing the continuous femtosecond oscillation regime, the stable locking of frequencies ($f_1 = f_2$) is preserved within the second region. Thus, in the second region one can observe a hysteresis in the dependence of $f_2 - f_1$ on Δx, which manifests itself in the existence of a bistable state at a fixed value of Δx, so that the laser switches into a specific state depending on how the transition from the first region to the second one occurs.

A similar effect of pulling takes place in the case of the automatic initiation of femtosecond oscillation in the third region. In the case of a transition from the second region without disruption of the current regime, the Ti:sapphire oscillator continues to operate in the pulsed regime due to the Kerr nonlinearity of the active medium crystal, while the nonlinear interaction between the pulses of the pump and oscillation in the crystal becomes weak because of their time mismatch. This regime of the Ti:sapphire laser operation is similar to the regime of continuous-wave pumping. In this case, no effect of the cavity length difference Δx on the radiation parameters exists. In the case of a transition to the third region with disruption of the pulsed oscillation regime of the Ti:sapphire laser, no automatic restart of the pulsed regime is observed. The laser oscillation in this case is continuous-wave and possesses the amplitude modulation at the frequency f_2, the modulation depth increasing with decreasing Δx.

From Fig. 3 one can see that the PRR locking occurs spontaneously with increasing cavity length of the Ti:sapphire laser at the positive frequency difference $f_2 - f_1 \approx 20$ Hz (point 1 in Fig. 3 that determines the left-hand boundary of the first region). With further elongation of the cavity (growth of Δx), the frequency locking of f_2 to f_1 is present till the right-hand boundary of the first region (point 2) and further to point 3, which is the right-hand boundary of the second region. At point 3, the enforced failure of lock-in (transition to point 4) occurs because of Δx reaching its critical value. In the course of backward motion, the PRR locking (point 5) occurs at Δx, close by the absolute value to the value of the detuning for the forward motion. Thus, points 1 and 5 determine the boundaries of the first region ($\Delta x_1, \Delta x_5$). The hysteresis similar to that in the course of cavity elongation is

observed between points 6 and 7 up to the breakdown of PRR locking at point 8 that occurs for the critical value of the detuning in the process of cavity shortening. The region of automatic re-initiation of the femtosecond oscillation (the second region) has the characteristic dimension of tens of micrometres, which in our case varied from 8 to 50 μm depending on the length of the used Ti:sapphire crystal and the tuning of the cavity of the synchronously pumped laser. From Fig. 3 it is seen that the general picture of the laser operation regimes can be asymmetric with respect to the critical values of Δx. Note that this asymmetry depends strongly on the alignment of the Ti:sapphire laser cavity.

We found two factors that determine the range of acceptable detuning $\Delta x_5 \div \Delta x_1$, within which the locking of the frequency f_1 occurs. On the one hand, it is the spatial overlap of the beam waists of the pump and Ti:sapphire laser cavity modes in the active medium of the Ti:sapphire laser. On the other hand, it is the net group velocity dispersion of its cavity. The overlap of the beam waists in the crystal of the active medium affects both the efficiency of the Kerr lensing and strength of the XPM effect, which affects the PRR locking. The introduction of a hard aperture into the Ti:sapphire laser cavity not only changes the dynamics of pulse formation, making the passive mode-locking regime more stable, but also significantly decreases the efficiency of cross-phase modulation, responsible for the effect of pulse synchronisation of the Ti:sapphire laser and its pump.

The matching of the pump and cavity mode beams in the Ti:sapphire crystal allows the variation in the locking region length, i.e., the quantity $\Delta x_5 - \Delta x_1$ that determines the stability of PRR locking with respect to the external environment factors. The variants of the Ti:sapphire laser cavity tuning are possible, for which the maximal change in the wavelength, arising in response to an increase in Δx, amounts to only 3–4 nm or 40–45 nm. In the latter case under the favourable external conditions (particularly, the constant ambient temperature), the locking is continuously maintained during six hours and longer.

The second important parameter affecting $\Delta x_5 - \Delta x_1$ and, therefore, the stability of the lasers synchronisation, is the net dispersion of the Ti:sapphire laser cavity that determines the pulse duration. The observed dependence agrees with expression (3), namely, the size of the region $(\Delta x_1, \Delta x_5)$ increases with increasing amount of the negative dispersion of the cavity. The increase in the net negative cavity dispersion and the accompanying increase in the oscillation pulse duration, in spite of decreasing the generated field intensity, only improve the locking stability. The amount of the negative dispersion also determines the proportionality factor between the cavity length mismatch Δx and the shift of the centre wavelength of the oscillation spectrum (the slope of the straight line in Fig. 4).

Our simplified model also shows that an increase in the pump pulse duration should positively affect the synchronisation stability; however, the experimental confirmation of this fact is presently absent.

4.2. Correlation experiment

In the course of the first experiment (see Fig. 2), the correlation function of the pulses of the Ti:sapphire laser and the pump laser was measured. To evaluate the quality of synchronisation of the laser pulses, we compared the measured correlation function (Fig. 5) with the convolution of the model Gaussian pulse and the soliton-like pulse, modelling the pulses of the Ti:sapphire laser and its pump, respectively. As seen from Fig. 5, the calculated and the experimental correlation function almost coincide: the widths of the peaks at the half-maximum level differ by 1.2 fs only, which is within the measurement error of the correlator (±1 fs). Thus, the average jitter value, measured within the range of delays available with the correlator (~6 ps), amounts to ~1 fs on the obserevation time scale exceeding hundreds of milliseconds.

The second experiment was carried out to determine the timing jitter on the observation time scale of 10 μs–1 s. In the course of the experiment, using the cross-correlation scheme and a digital oscilloscope we directly recorded the amplitude of fluctuations. The delay line DL was fixed in the position corresponding to the overlap of the pulse envelopes at the level of half their amplitude (horizontal line in Fig. 5). Provided that the jitter is small compared to the pulses duration, the intensity of the signal at the sum optical frequency can be recalculated into the jitter amplitude via the derivative of the correlation function with respect to the delay time.

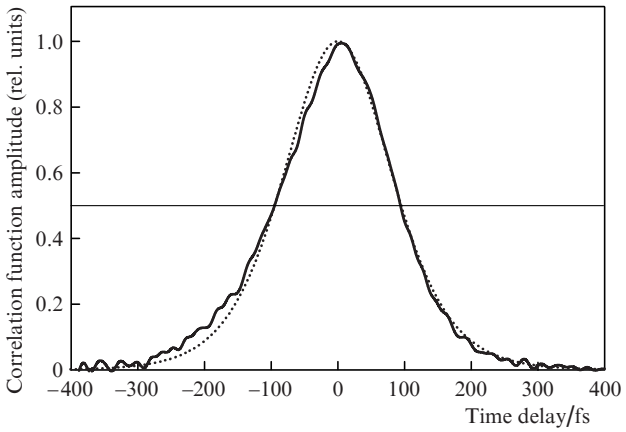

Figure 5. Experimental intensity correlation function for pulses of the ytterbium laser and the Ti:sapphire laser (the half-maximum width 188.8 fs) (solid line) and the calculated correlation function of the Gaussian pulse and the soliton with the parameters, corresponding to the measured ones for the Ti:sapphire laser and the ytterbium one (the half-maximum width 190.0 fs) (dotted line).

The normalised spectral densities of the power of the measured fluctuation signal and the intrinsic noises of the measuring system are presented in Fig. 6. The low frequency (with the frequency below 1 Hz) components, related to the variations in the optical breadboard of the system due to the changing temperature of water in the cooling circuit, are removed from the spectra. The low frequency oscillations can be physically eliminated by using a more advanced system of thermal stabilisation (e.g., based on Peltier elements instead of the refrigerator system).

The comparison of the jitter spectra and the intrinsic noise of the measuring system shows that the major part of the fluctuation power belongs to the spectral range 1 Hz – 25 kHz. In the low-frequency region (1–100 Hz) the power spectral density decreases as $1/f$, and in the region 20–25 kHz becomes smaller than the detection system noise floor.

The root-mean-square amplitude of the jitter in the range 1 Hz – 20 kHz was estimated by integrating the recorded

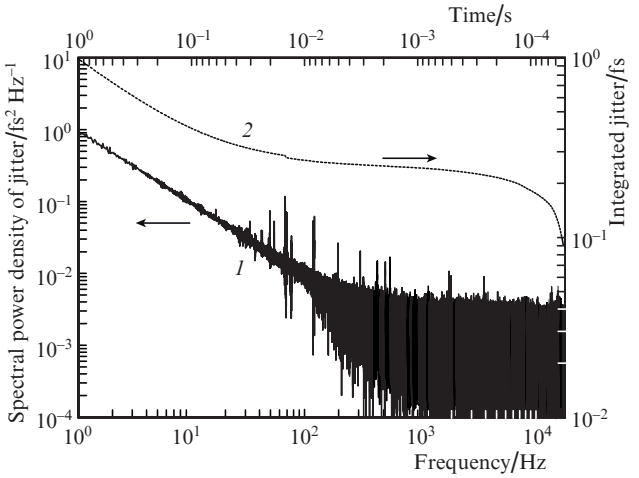

Figure 6. (*1*) Spectral power density of temporal fluctuations and (*2*) the dependence of root-mean-square amplitude of fluctuations on the observation time.

spectral data. In Fig. 6, curve (*2*) shows the integral value of the timing jitter as a function of the observation time, obtained by integrating the power spectral density. Since the data acquisition time by the oscilloscope in the second experiment was only 1 s, the root-mean-square amplitude of the timing jitter between two laser pulse trains resulted in a value slightly less than 1 fs.

5. Conclusions

We have constructed a laser system consisting of two solid-state laser oscillators with timing accuracy of 1 fs. A qualitative model is proposed to explain the effect of PRR locking, and to describe the regimes of the Ti:sapphire laser operation as functions of the mismatch between its cavity length and that of the pump laser.

Due to the nonlinear coupling of pump and oscillation pulses in the active medium of the Ti:sapphire laser through cross-phase modulation, the pulse repetition rate of the Ti:sapphire laser exactly matches the pulse repetition rate of the pump pulses. This effect takes place at the expense of shifting the oscillation spectrum and the corresponding change in the pulse group velocity inside the cavity. This PRR locking mechanism allows one to avoid the use of any additional electronics.

The synchronous pumping of one oscillator by another allows stable and exact locking of the pulse repetition rate of the pumped oscillator to the repetition rate of the pump pulses. In the frequency band 1 Hz – 250 kHz, the dominant part of the timing jitter spectral power lies within the acoustic range 1 Hz – 10 kHz. The obtained estimate of the root-mean-square amplitude of the timing jitter, since it takes into account also all mechanical vibrations of the system casing and individual elements both inside and outside it (in particular, the elements of the jitter measurement system), is the upper estimate.

The locking stability of the oscillators is critically affected by the tuning of the Ti:sapphire laser cavity and the dispersion conditions for the oscillation pulse in the cavity. The choice of the active medium crystal length, the overlap of the cavity mode and the pump mode within the Ti:sapphire crystal and the tuning of the oscillator compressor allow stable locking of the pulse repetition rate that lasts for 3–6 hours without any external compensation for the action on the system and its elements.

Based on the presented scheme, we have constructed a prototype system of synchronised oscillators with a feedback mechanism based on a Ti:sapphire spectrum shift. The active tuning of the cavity length of the Ti:sapphire laser allows increasing the time of continuous PRR-locked operation of two lasers from 3–6 hours to 12 hours and more. The nonlinear coupling in the crystal of the synchronously pumped oscillator again provides the synchronous operation of the two lasers in the prototype system, with the electronic feedback system introducing just occasional corrections of the cavity length in one of the lasers in order to support the optimal conditions for maintaining the frequency locked operation. The principle of operation and the invention prototype are described in more detail in the application for the Russian Federation Patent 2016121460/28(033586).

The system can be considered as an alternative to the oscillators based on the Ti:sapphire crystal with continuous-wave pumping. The abovementioned advantages compared to the Ti:sapphire oscillators with a traditional pumping scheme make such a system promising from the point of view of applications, particularly, in the spectroscopy with high temporal resolution [25, 26], in the optical frequency metrology [27], and for direct optical synthesis of ultra-wideband pulses [28]. The latter is possible using the well-approved traditional methods of phase stabilisation of the light field of the pulses in each of the laser channels, frequency-locked by means of the proposed method.

References

1. Leitenstorfer A., Fürst C., Laubereau A. *Opt. Lett*., **20** (8), 916 (1995).
2. Wei Z., Kobayashi Y., Zhang Z. *Opt. Lett*., **26** (22), 1806 (2001).
3. Betz M., Sotier F., Tauser F. *Opt. Lett*., **29** (6), 629 (2004).
4. Seitz W., Schibli T.R., Morgner U. *Opt. Lett*., **27** (6), 454 (2002).
5. Ma L.-S., Shelton R.K., Kapteyn H.C. *Phys. Rev. A*, **64**, 021802(R) (2001).
6. Shelton R.K., Foreman S.M., Ma L.-S. *Opt. Lett*., **27** (5), 312 (2002).
7. Kim E.B., Lee J., Trung L. *Opt. Express*, **17** (23), 20920 (2009).
8. Kubota H., Kurokawa K., Nakazawa M. *Opt. Lett*., **13** (9), 749 (1988).
9. Stamm U., Weidner F. *Opt. Commun*., **71** (3,4), 165 (1989).
10. Churin D., Olson J., Norwood R.A. *Opt. Lett*., **40** (11), 2529 (2015).
11. Kobtsev S., Kukarin S., Kokhanovskiy A. *Opt. Express*, **23** (14), 18548 (2015).
12. Ell R., Angelow G., Seitz W. *Opt. Express*., **13** (23), 9292 (2005).
13. Siders C.W., Gaul E.W., Downer M.C. *Rev. Sci. Instrum*., **65**, 3140 (1994).
14. Spielmann Ch., Krausz F., Brabec T. *Opt. Lett*., **16** (15), 1180 (1991).
15. Borisevich N.A., Buganov O.V., Tikhomirov S.A. *Kvantovaya Elektron*., **23** (11), 1003 (1996) [*Quantum Electron*., **26** (11), 978 (1996)].
16. Borisevich N.A., Buganov O.V., Tikhomirov S.A. *Kvantovaya Elektron.*, **28** (3), 225 (1999) [*Quantum Electron*., **29** (9), 780 (1999)].
17. Liu J., Wang W.W., Liu C.C. *Laser Phys. Lett*., **7** (2), 104 (2010).
18. Pronin O., Brons J., Grasse C. *Opt. Lett*., **36** (24), 4746 (2011).
19. Ashkin A., Gordon J.P. *Opt. Lett*., **8** (11), 511 (1983).
20. Wei Z., Kaboyashi Y., Torizuka K. *Appl. Phys. B*, **74** (1), S171 (2002).
21. Yoshitomi D., Kobayashi Y., Kakehata M. *Opt. Lett*., **31** (22), 3243 (2006).

22. Pe'er A., Bromberg Y., Dayan B. *Opt. Express*, **15** (14), 8760 (2007).
23. Okamoto H., Tasumi M. *Rev. Sci. Instrum.*, **66** (11), 5165 (1995).
24. Chesnoy J., Fini L. *Opt. Lett.*, **11** (10), 635 (1986).
25. Stolow A., Bragg A.E., Neumark M. *Chem. Rev*., **104**, 1719 (2004).
26. Feldmann J., Cundiff S.T., Arzberger M. *J. Appl. Phys*., **89**, 1180 (2001).
27. Diddams S.A., Jones D.J., Ye J. *Phys. Rev. Lett*., **84** (22), 5102 (2000).
28. Cundiff S.T., Ye J., Hall J.L. *Rev. Sci. Instrum*., **72** (10), 3749 (2001).